北京大學
地球物理学系

Numerical Modeling of Global Seismic Wave Propagation in the Whole Mars Models and Effect of Lateral Crustal Variation

Yanbin Wang, Wanbo Xiao, Di Deng

Department of Geophysics, School of Earth and Space Sciences, Peking University

PS4.1, EGU General Assembly 2020, May 4, 2020

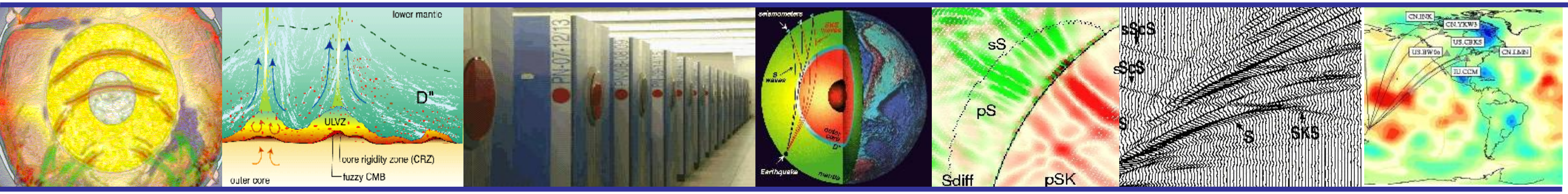

- Background
- PSM/FDM hybrid modeling method
- Global P-SV and SH wave propagation
- Effect of lateral variation of Martin crust thickness
- Discussion and conclusions

Background

- Seismological methods played import roles in the study of the Earth and Moon’s interior.
- The InSight Spacecraft landed on Mars on November 26, 2018 and installed the first seismometer on Mars. It provides the in situ observation of interior structure and seismic activity of Mars for the first time.
- Numerical modeling of seismic wave propagation in the whole Mars models plays important roles in understanding the generation and propagation of various seismic phases in the Mars.
- Numerical modeling helps to analyze the effects of lateral heterogeneous crust and depth of core mantle boundary on seismic wave propagation in Mars.

PSM/FDM hybrid modeling method

$$\rho\frac{\partial v_r}{\partial t}=\frac{1}{r}\frac{\partial}{\partial r}(r\sigma_{rr})+\frac{1}{r}\frac{\partial\sigma_{r\theta}}{\partial\theta}-\frac{\sigma_{\theta\theta}}{r}+f_r$$

$$\rho\frac{\partial v_\theta}{\partial t}=\frac{1}{r^2}\frac{\partial}{\partial r}(r^2\sigma_{r\theta})+\frac{1}{r}\frac{\partial\sigma_{\theta\theta}}{\partial\theta}+f_\theta$$

$$\rho\frac{\partial v_z}{\partial t}=\frac{\partial\sigma_{zr}}{\partial r}+\frac{1}{r}(\frac{\partial\sigma_{z\theta}}{\partial\theta}+\sigma_{zr})+f_z$$

$$\frac{\partial\sigma_{rr}}{\partial t}=(\lambda+2\mu)\frac{\partial v_r}{\partial r}+\frac{\lambda}{r}(\frac{\partial v_\theta}{\partial\theta}+v_r)$$

$$\frac{\partial\sigma_{\theta\theta}}{\partial t}=\lambda\frac{\partial v_r}{\partial r}+(\frac{\lambda+2\mu}{r})(\frac{\partial v_\theta}{\partial\theta}+v_r)$$

$$\frac{\partial\sigma_{r\theta}}{\partial t}=\mu\frac{\partial v_\theta}{\partial r}+\frac{\mu}{r}\left(\frac{\partial v_r}{\partial\theta}-v_\theta\right)$$

$$\frac{\partial\sigma_{zr}}{\partial t}=\mu\frac{\partial v_z}{\partial r}$$

$$\frac{\partial\sigma_{z\theta}}{\partial t}=\frac{\mu}{r}\frac{\partial v_z}{\partial\theta}$$

Wave equations (Wang et al., 2013)

PSM/FDM hybrid modeling method

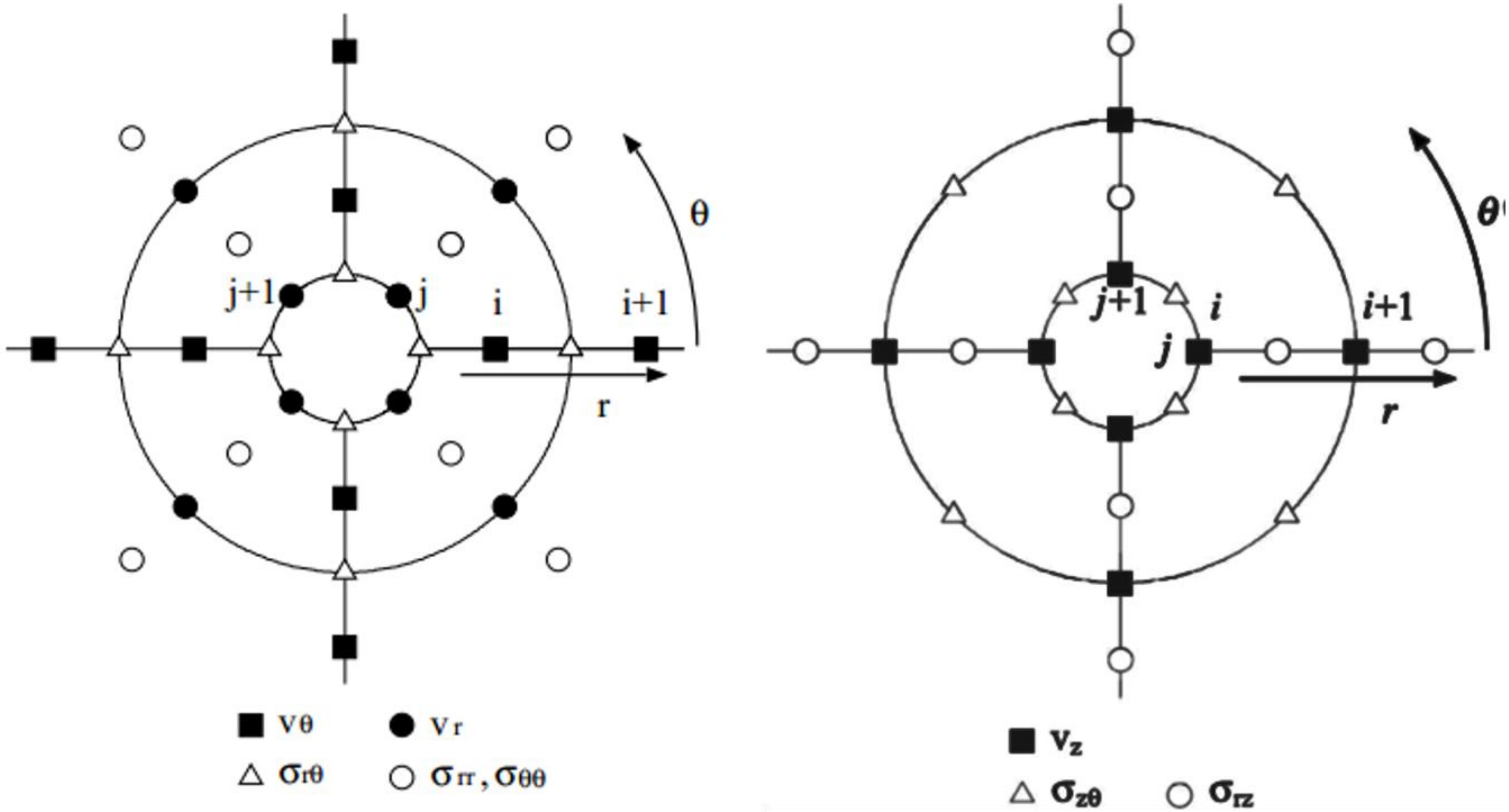

Staggered grid configuration (Wang et al., 2013)

Global P-SV and SH wave propagation

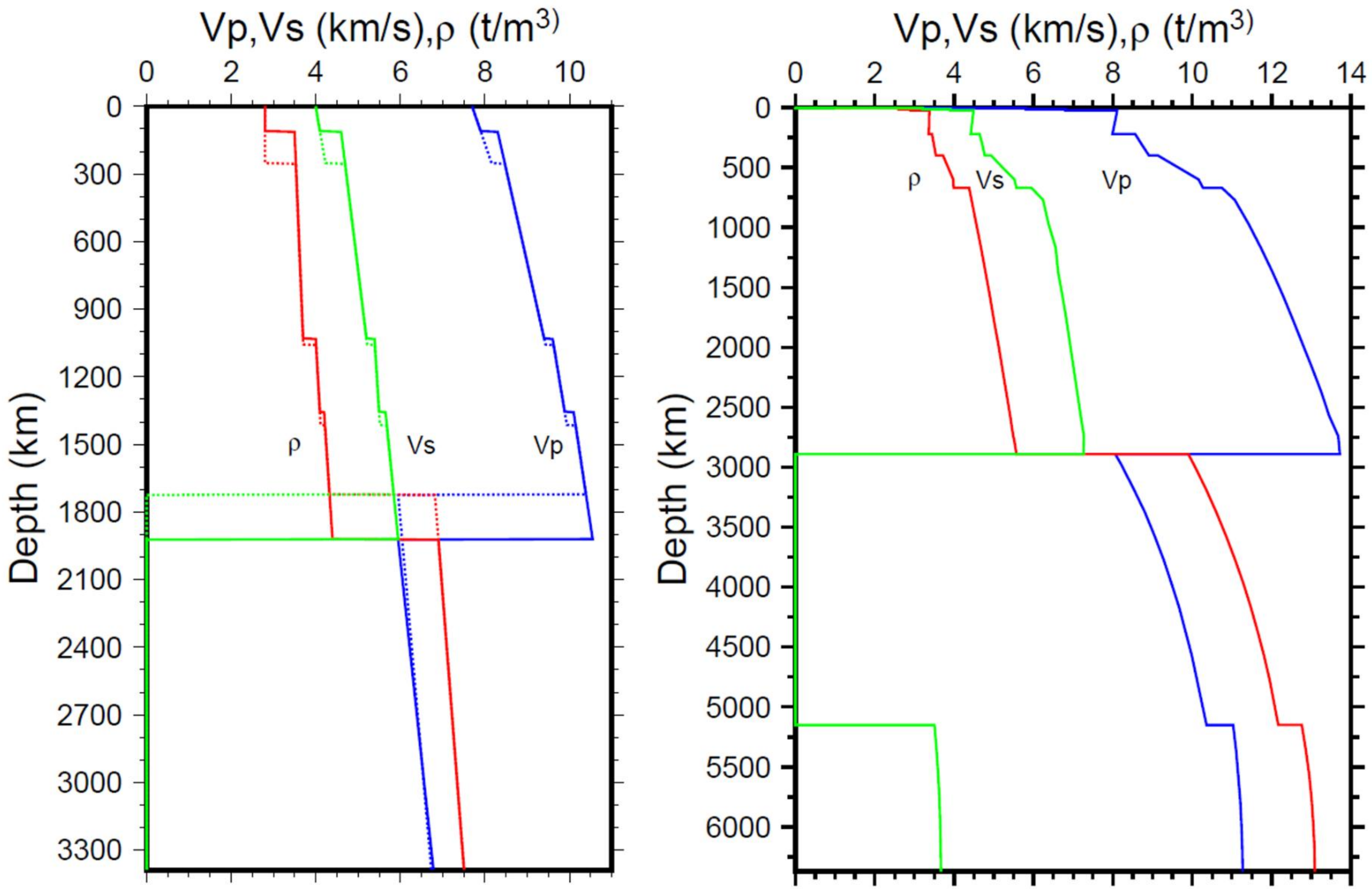

Left: The whole Mars models (model A: solid line, model B: dashed line) (Sohl and Spohn, 1997), Right: the whole Earth model (PREM) (Dziewonski and Anderson, 1981)

Global P-SV and SH wave propagation

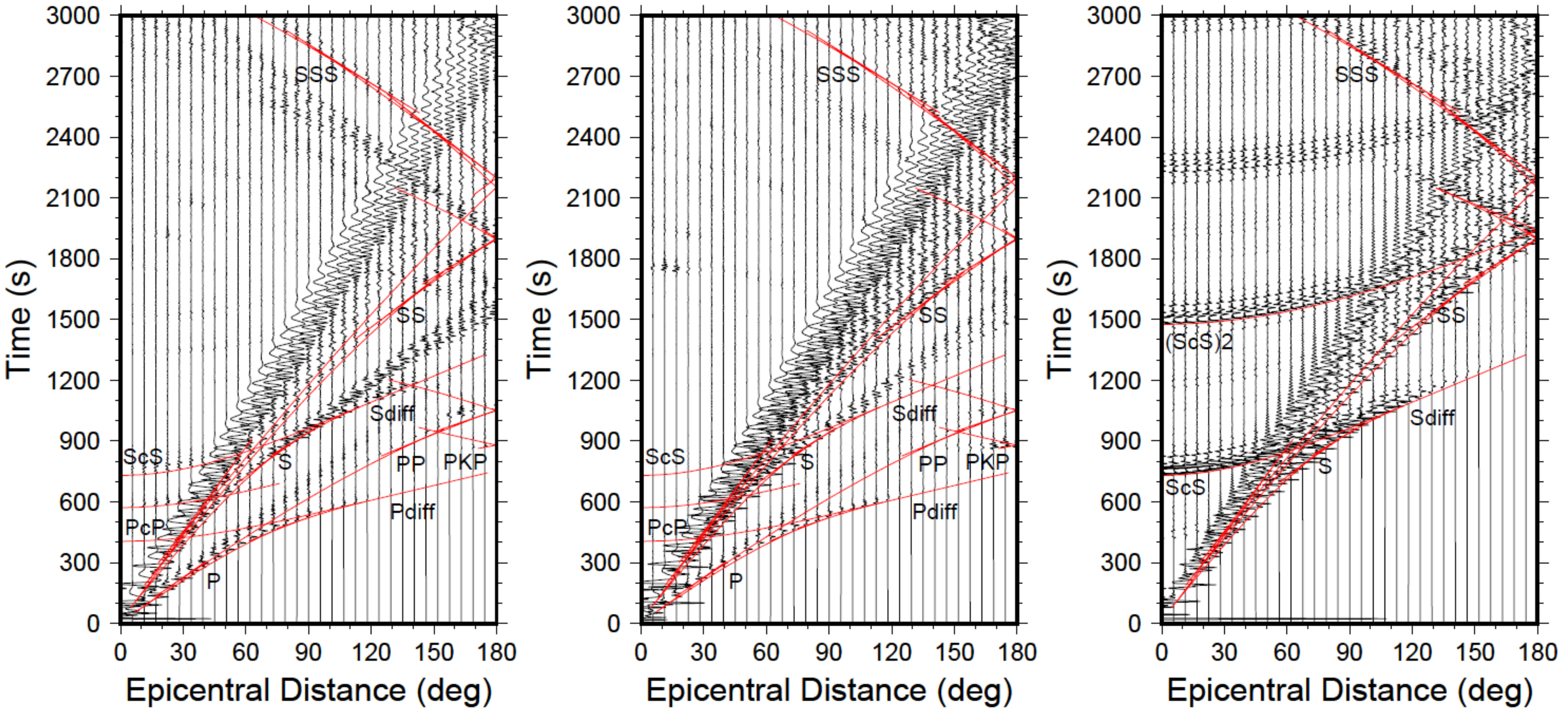

Synthetic displacement seismograms at Mars surface for a 60 km deep Marsquake for model A. From left to right are the radial, vertical and transverse component, respectively. Red curves show ray theoretical travel time for various seismic phases.

Global P-SV and SH wave propagation

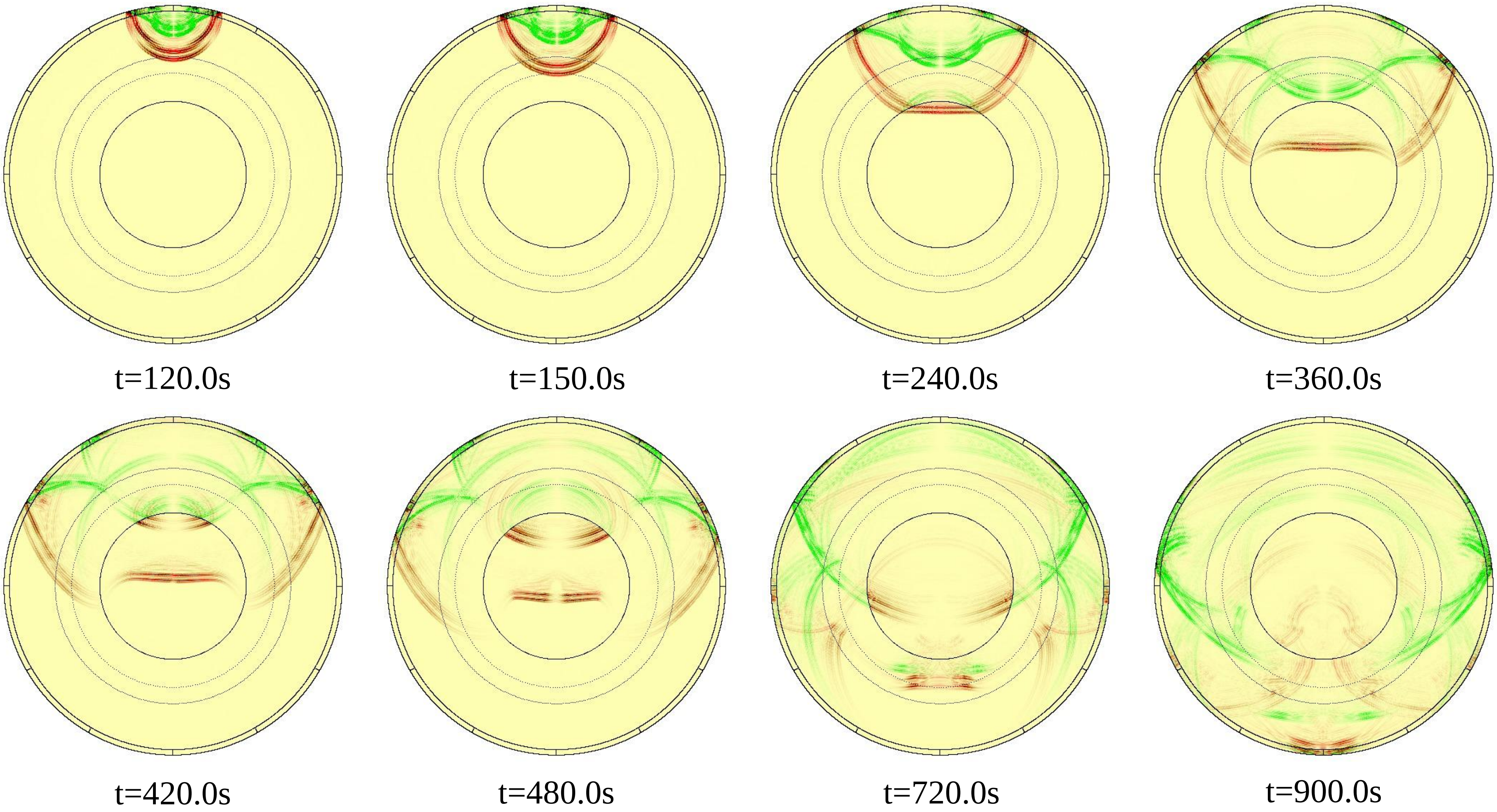

Wavefield snapshots calculated at 8 time steps for P- and SV-wave propagation in model A for a 60 km deep marsquake. Red and green show P- and SV-wave, respectively.

Global P-SV and SH wave propagation

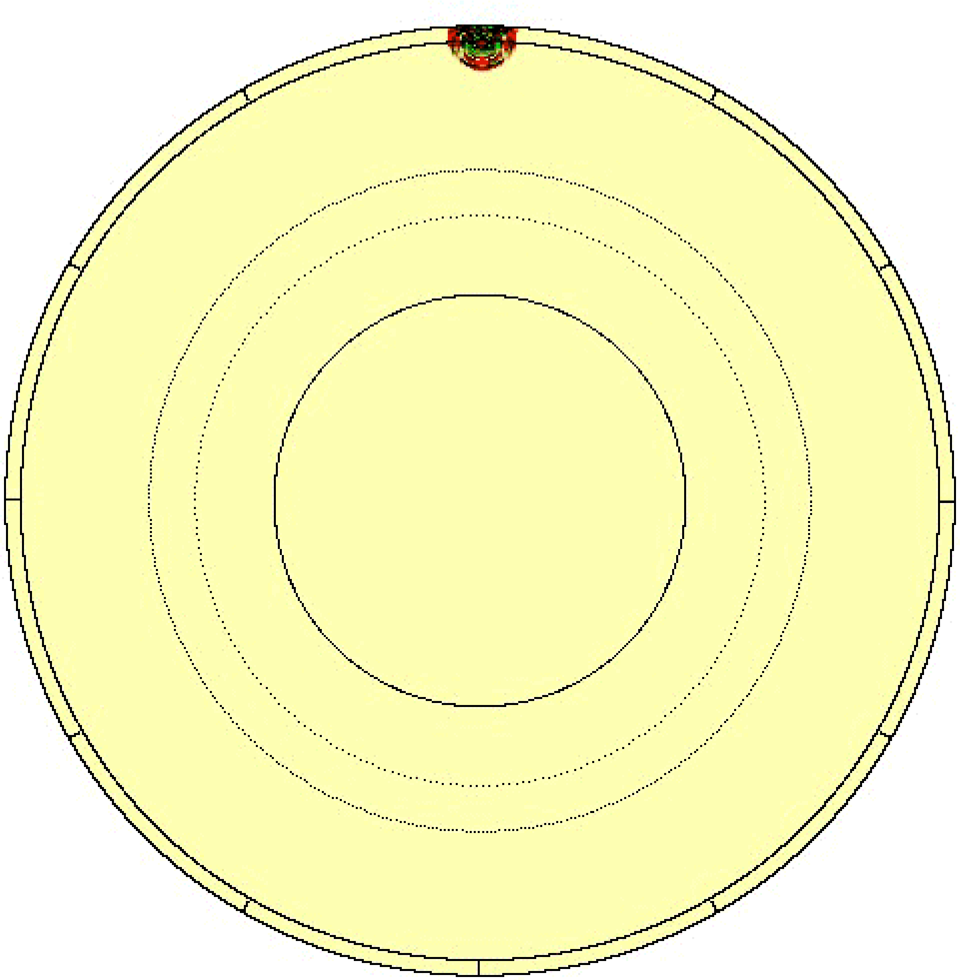

Global P- and SV-wave propagation in model A for a 60 km deep marsquake. Red and green show P- and SV-wave, respectively.

北京大学 地球物理学系

Global P-SV and SH wave propagation

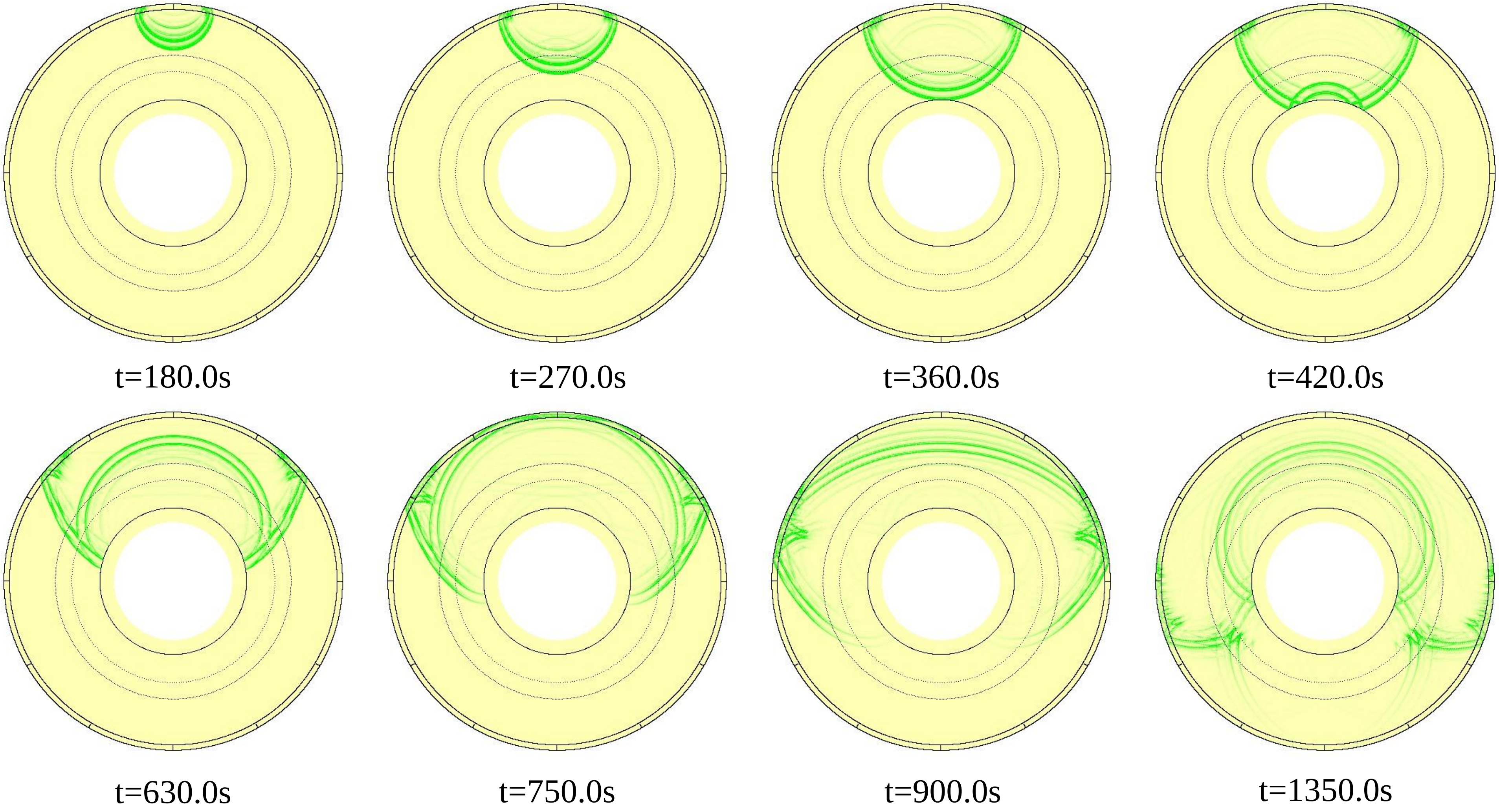

Wavefield snapshots calculated at 8 time steps for SH-wave propagation in model A for a 60 km deep marsquake.

Global P-SV and SH wave propagation

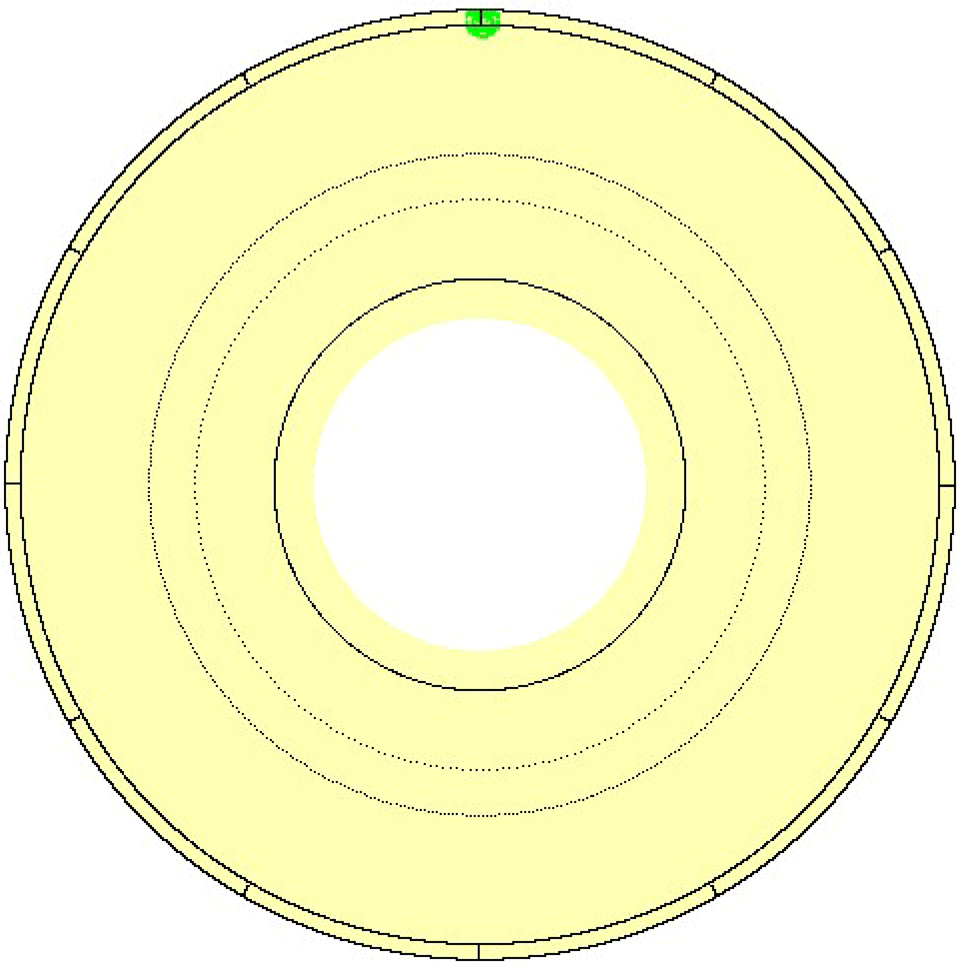

Global SH-wave propagation in model A for a 60 km deep marsquake.

Global P-SV and SH wave propagation

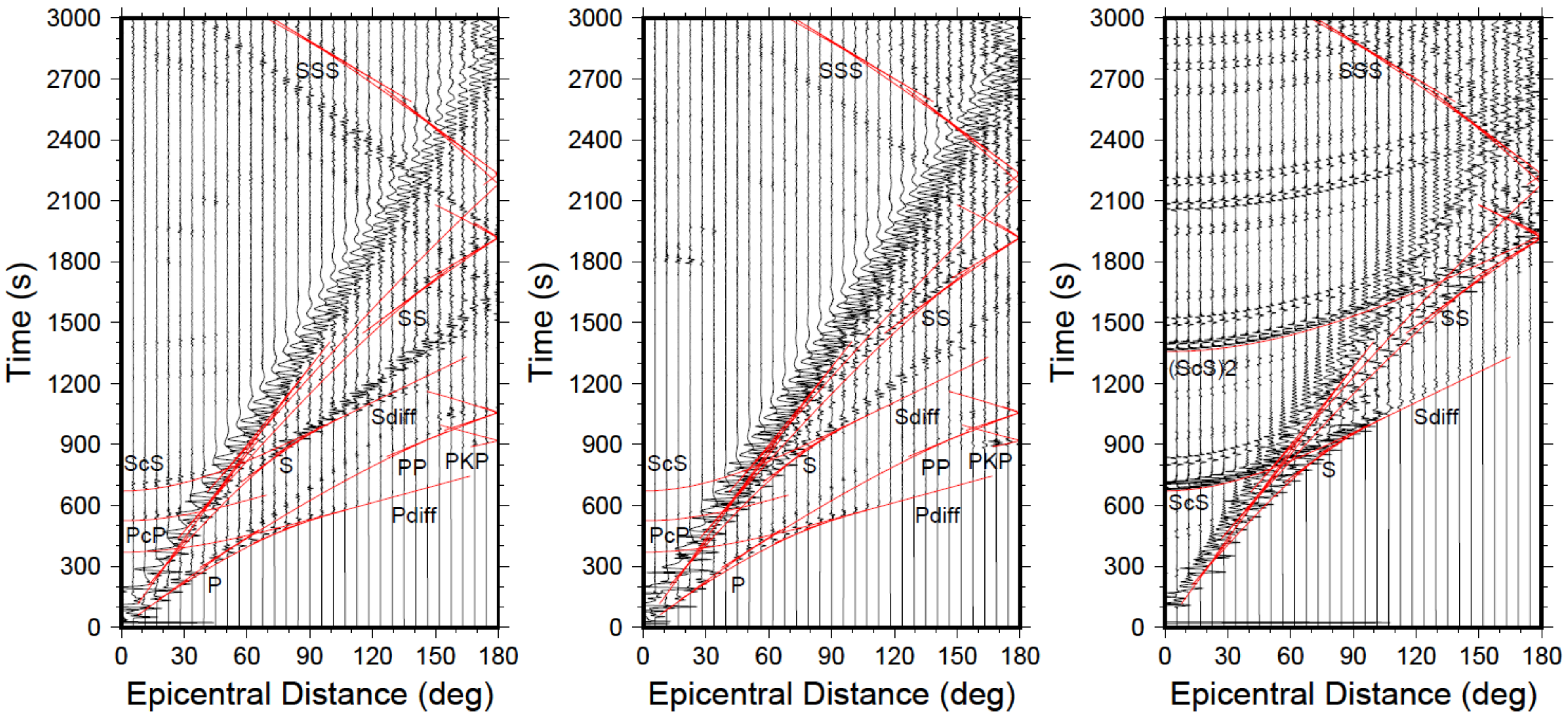

Synthetic displacement seismograms at Mars surface for a 60 km deep Marsquake for model B. From left to right are the radial, vertical and transverse component, respectively. Red curves show ray theoretical travel time for various seismic phases.

Global P-SV and SH wave propagation

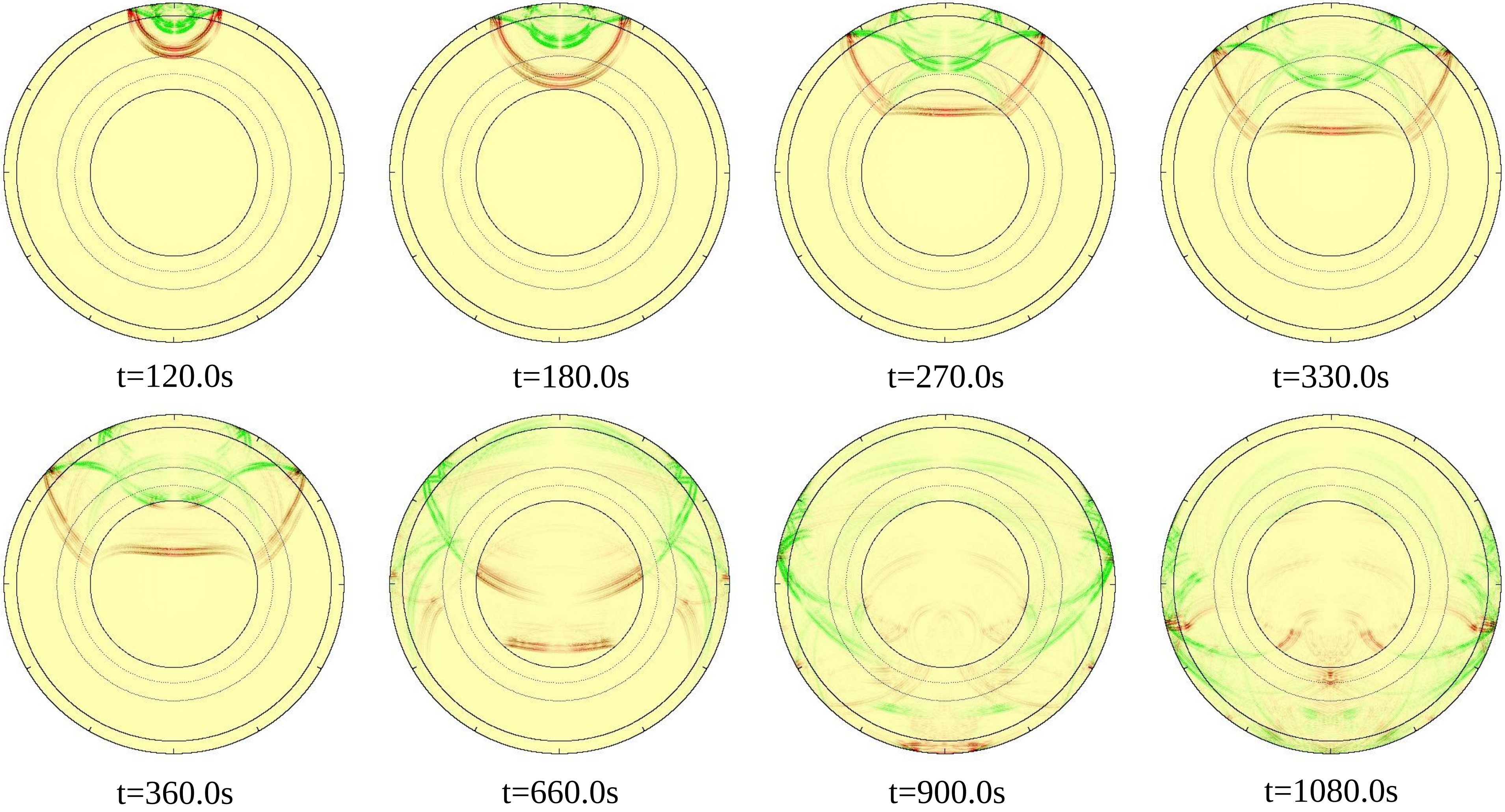

Wavefield snapshots calculated at 8 time steps for P- and SV-wave propagation in model B for a 60 km deep marsquake. Red and green show P- and SV-wave, respectively.

Global P-SV and SH wave propagation

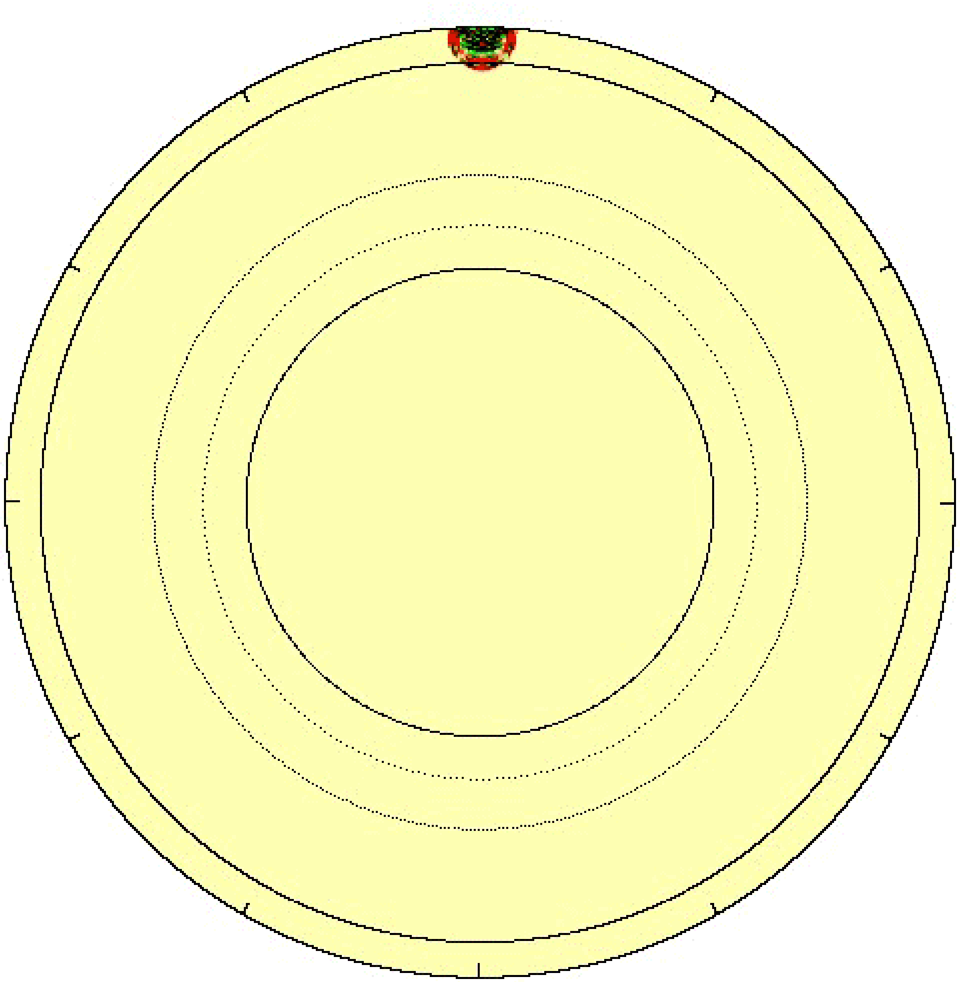

Global P- and SV-wave propagation in model B for a 60 km deep marsquake. Red and green show P- and SV-wave, respectively.

Global P-SV and SH wave propagation

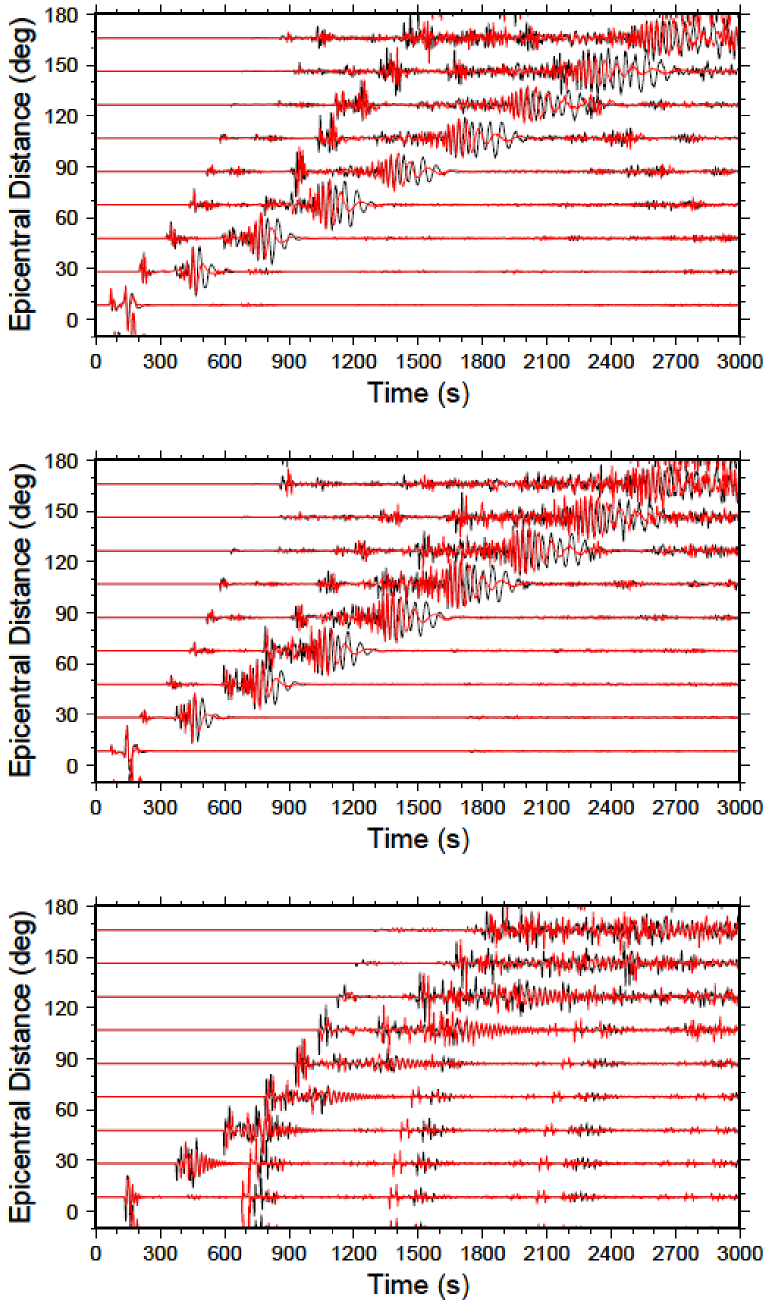

Comparison of synthetic seismograms between models A and B. From top to bottom are radial, vertical and transverse component, respectively. Black and red waveforms show results for model A and B, respectively.

Effect of heterogeneous Martin crust

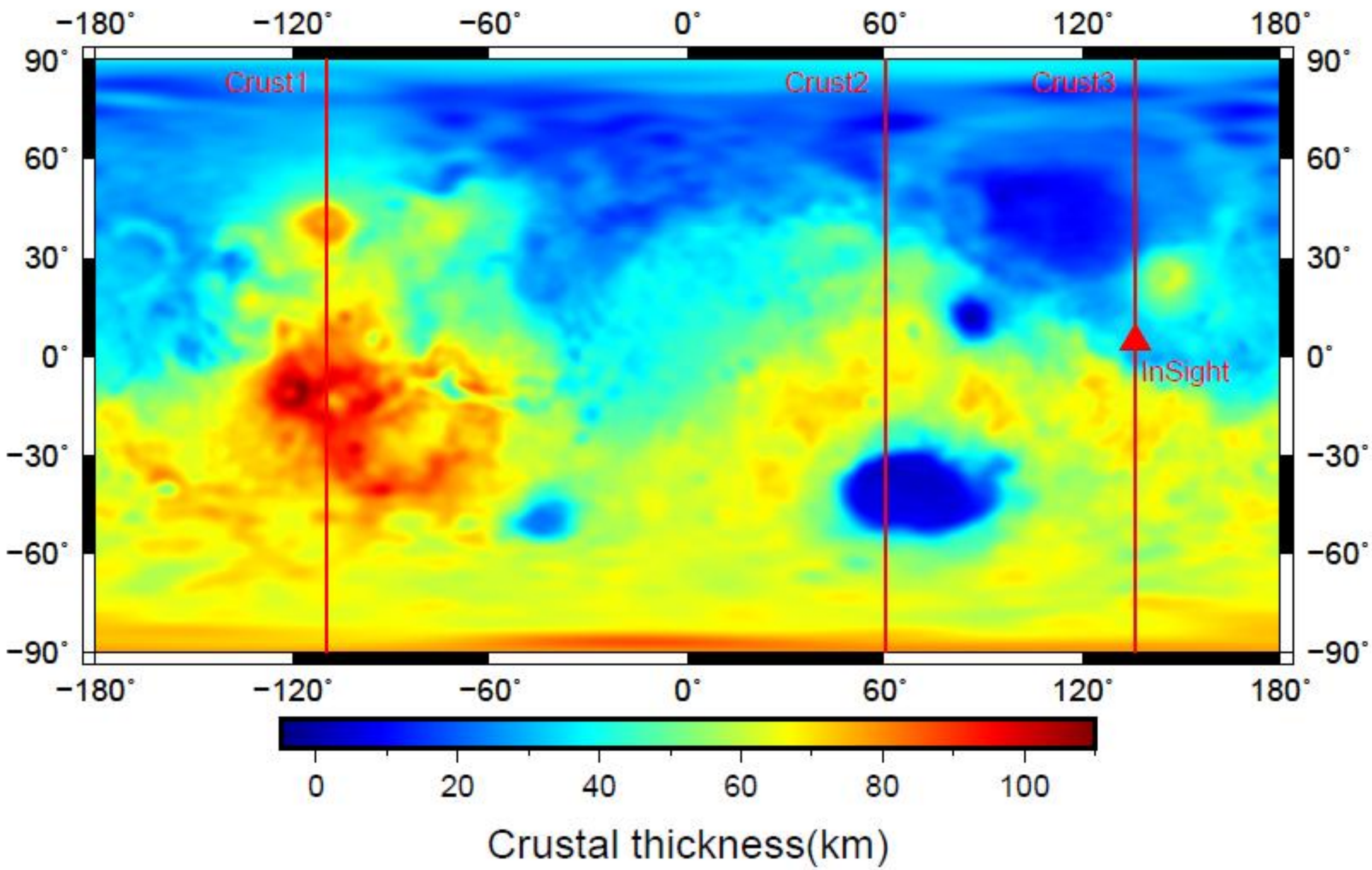

Global distribution of Martin crust thickness (Wieczorek and Zuber, 2004) and three profiles used in the modeling.

Global P-SV and SH wave propagation

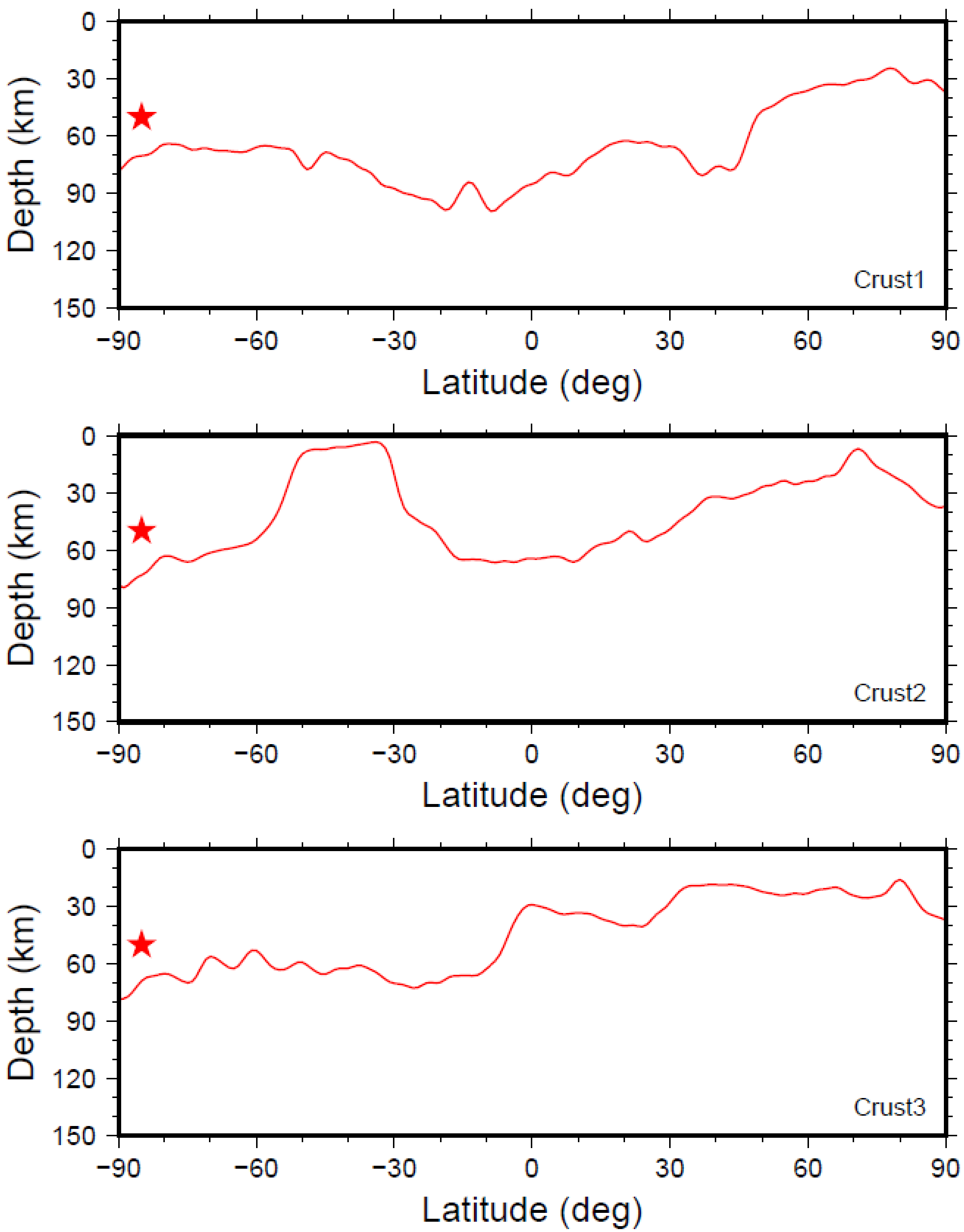

Three 2D Mars models with lateral variation of crust thickness. Red star is the location of marsquake source.

北京大学 地球物理学系

Effect of heterogeneous Martin crust

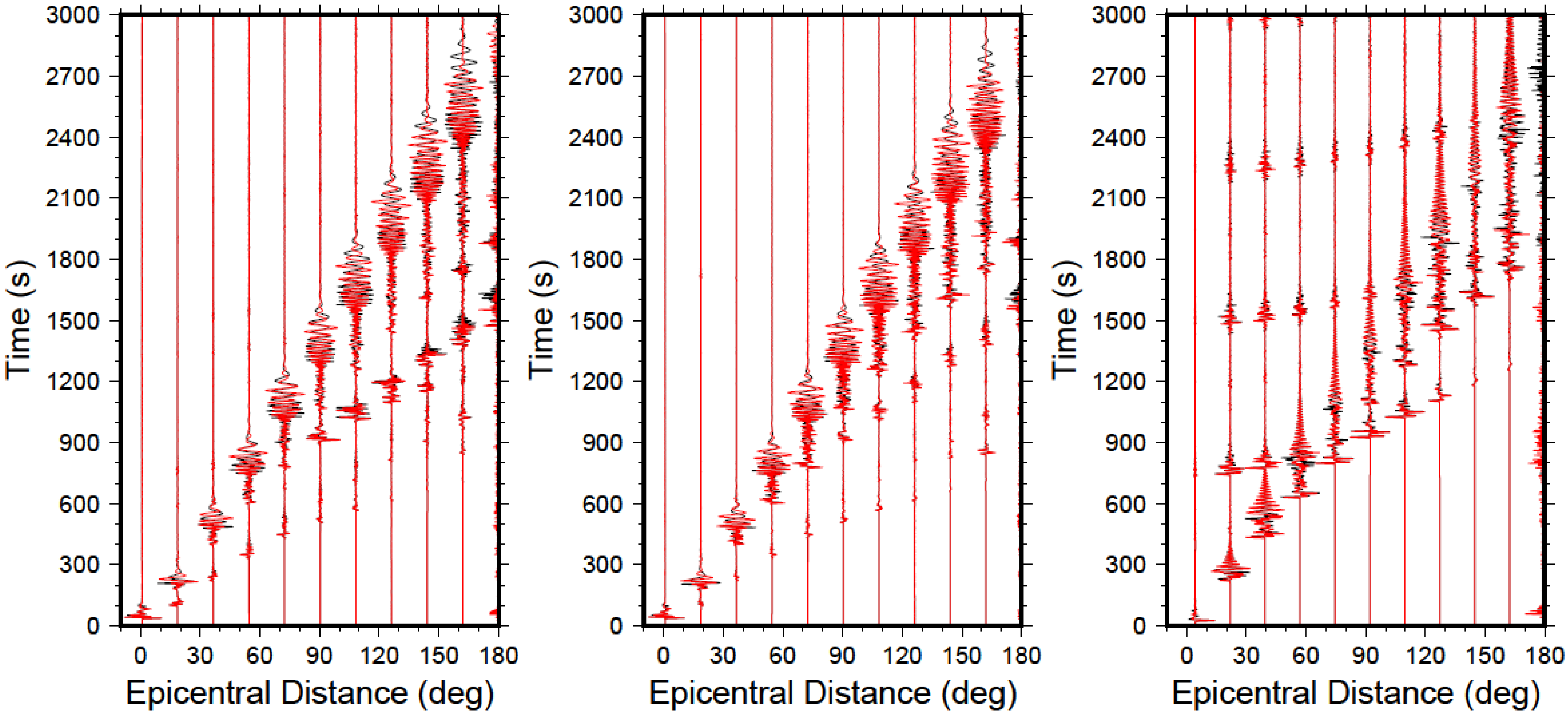

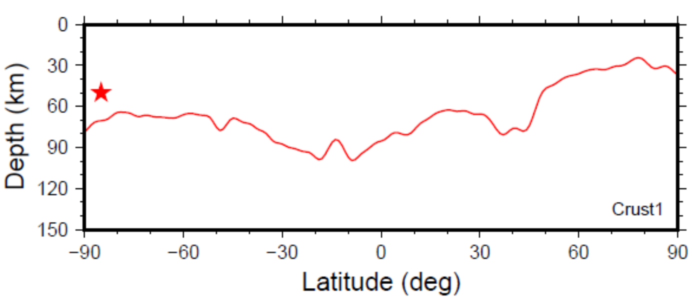

Comparison of synthetic seismograms for 2D model crust1 (red) and global model A (black). From left to right show radial, vertical and transverse component, respectively.

Effect of heterogeneous Martin crust

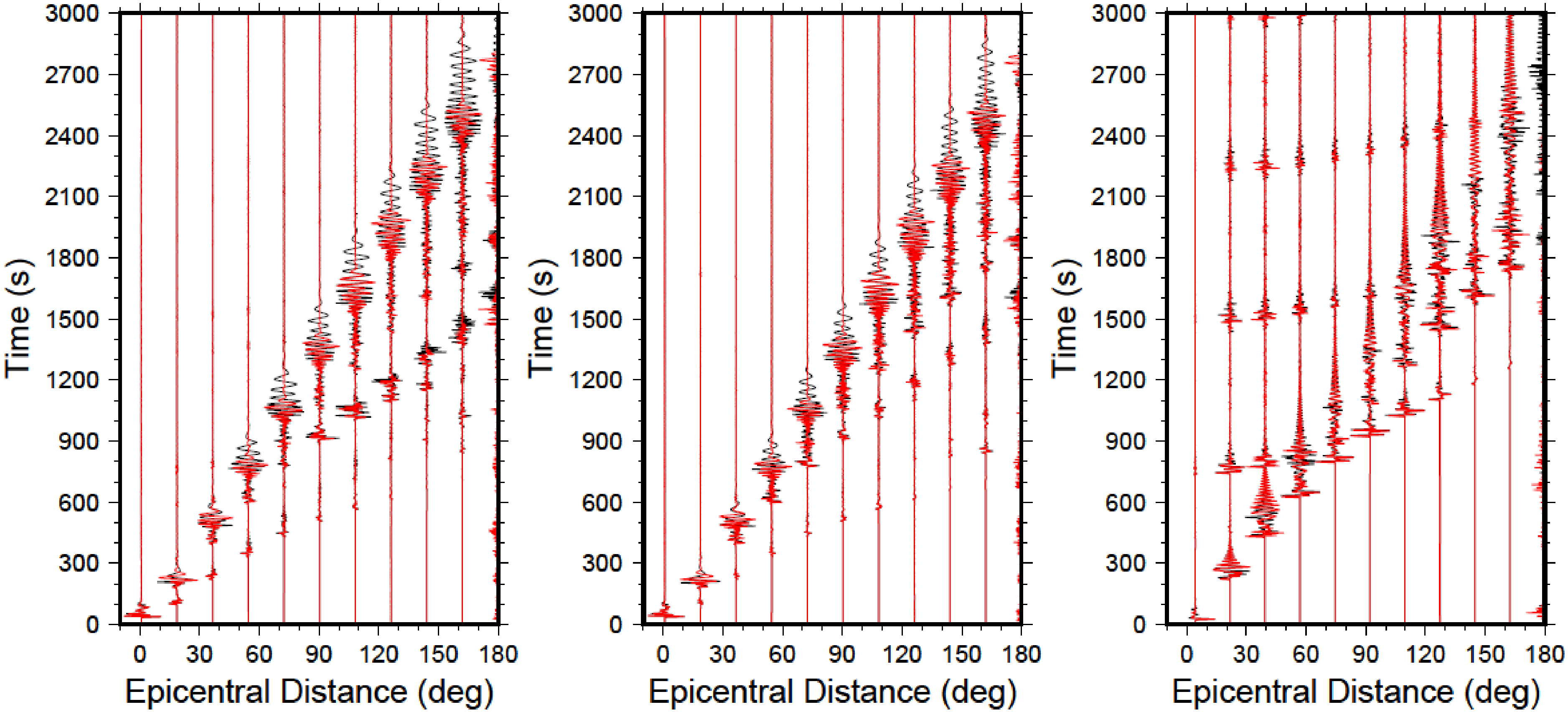

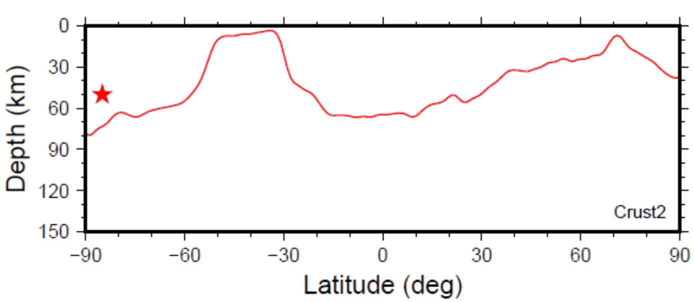

Comparison of synthetic seismograms for 2D model crust2 (red) and global model A (black). From left to right show radial, vertical and transverse component, respectively.

Effect of heterogeneous Martin crust

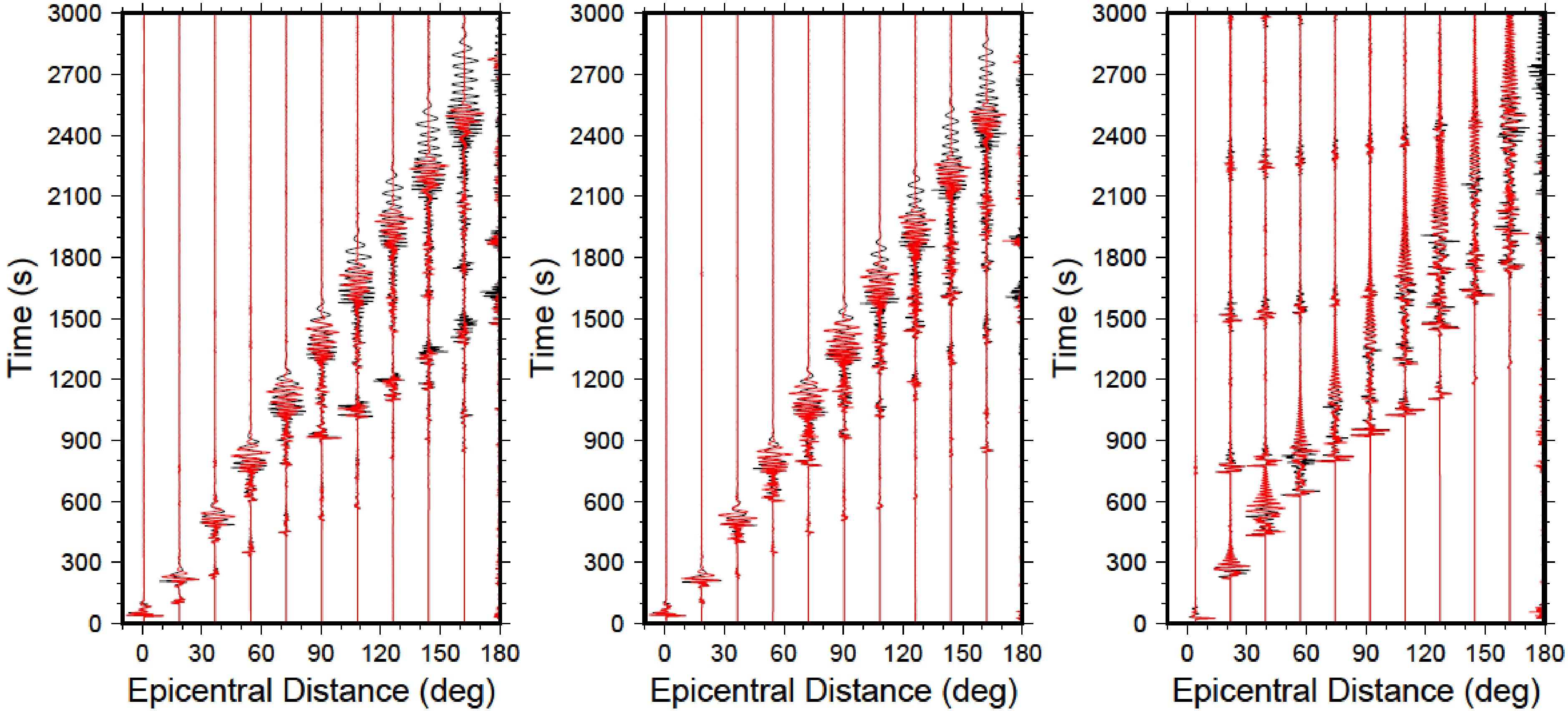

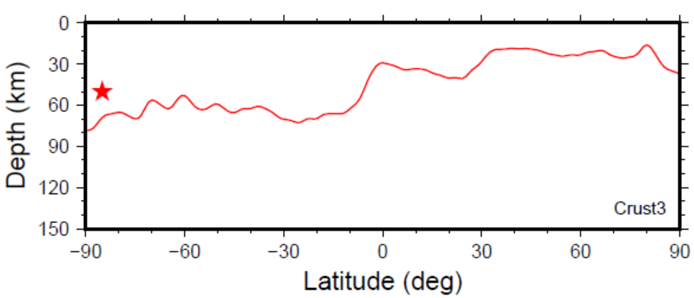

Comparison of synthetic seismograms for 2D model crust3 (red) and global model A (black). From left to right show radial, vertical and transverse component, respectively.

Effect of heterogeneous Martin crust

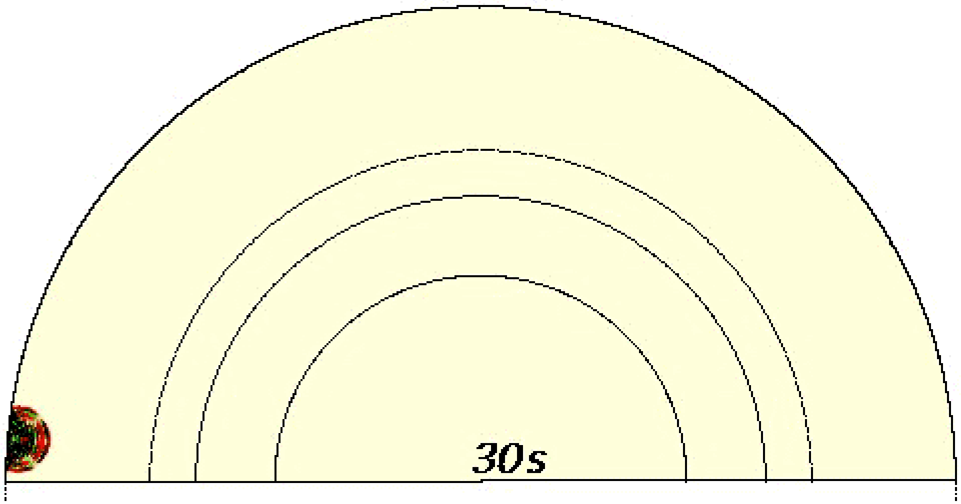

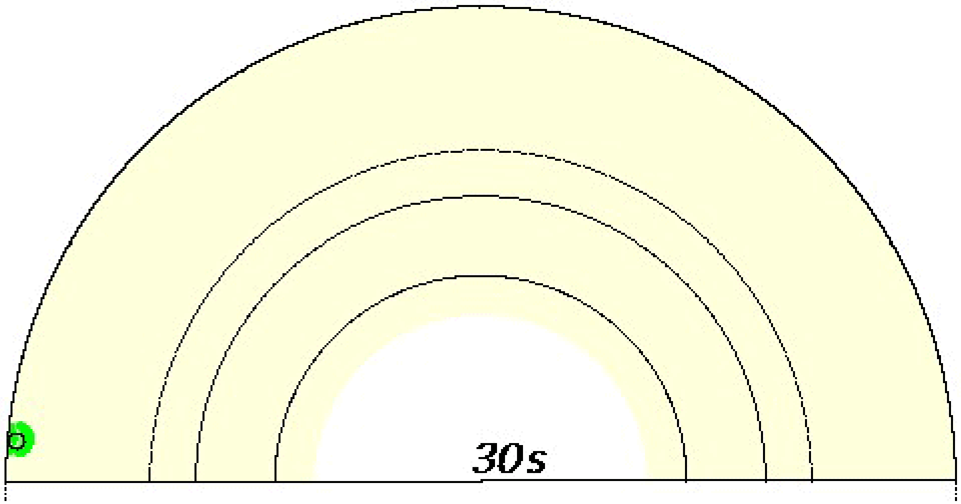

Global P- and SV-wave (top) and SH-wave (bottom) propagation in 2D model crust3 including InSight landing site for a 50 km deep marsquake. Red and green show P-, SV- and SH-wave, respectively.

Discussion and conclusions

We modeled global P-SV and SH wave propagation in the whole Mars model with staggered grid PSM/FDM hybrid method.

Modeling for two global models (Sohl and Spohn, 1997) show that multiple reflections and conversions of seismic waves and their constructive interference occurred inside the low-velocity Martian crust form reverberating wave trains. Thickness of Martian crust significantly affect the propagation of multiple surface reflections and surface waves.

Global wave propagation modeling show that seismic reflections from core-mantle boundary can be clearly identified from the calculated transverse component seismogram.

Based on Martian crustal thickness model (Wieczorek and Zuber, 2004), we simulate seismic wave propagation in laterally heterogeneous Martian crust and analyze its influence on global seismic wave propagation. Lateral variation of Martian crustal thickness has strong effect on the propagation of multiple surface reflections and surface waves.

Thank you！

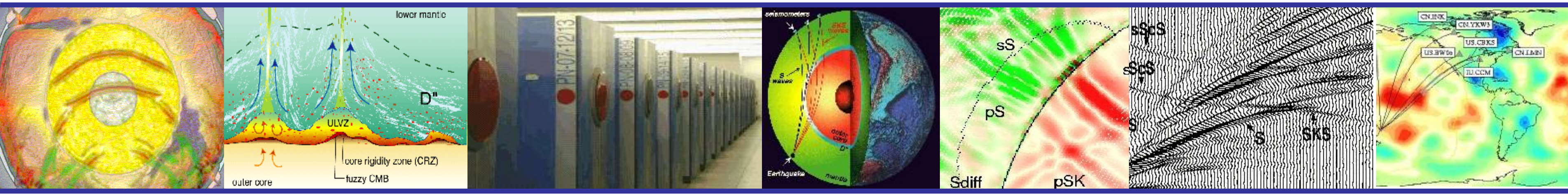
lower mantle
D"
ULVZ
core rigidity zone (CRZ)
fuzzy CMB
outer core
sS
pS
Sdiff
pSK
sScS
ScS
S
SKS